Shift of stereochemical nonrigidity from coordination units to polymethylene fragments in heterospin copper(II) hexafluoroacetylacetonate complexes with nitronyl nitroxide biradicals*

G. V. Romanenko,[a] S. E. Tolstikov,[a,b] E. V. Tretyakov,[a] S. V. Fokin,[a,b] V. N. Ikorskii,[a†] and V. I. Ovcharenko[a,b]★

[a]*International Tomography Center, Siberian Branch of the Russian Academy of Sciences, 3a ul. Institutskaya, 630090 Novosibirsk, Russian Federation*
Fax: +7 (383 2) 33 1399. E-mail: Victor.Ovcharenko@tomo.nsc.ru
[b]*Novosibirsk State University, 2 ul. Pirogova, 630090 Novosibirsk, Russian Federation*

The reactions of bis(hexafluoroacetylacetonato)copper(II) [$Cu(hfac)_2$] with the nitronyl nitroxide biradicals bis[4-(4,4,5,5-tetramethyl-3-oxide-1-oxyl-4,5-dihydro-1*H*-imidazol-2-yl)pyrazol-1-yl]alkanes (L^6, L^{10}, and L^{12}) produced the framework heterospin complex $[Cu(hfac)_2]_2L^6$ and the layer-polymeric heterospin complexes $[Cu(hfac)_2]_2L^{10}$ and $\{[Cu(hfac)_2]_2L^{12}\}[Cu(hfac)_2(Pr^iOH)_2]$, respectively. In the solid state of these compounds, the stereochemical nonrigidity is manifested as a deformation of the polymethylene fragments $—(CH_2)_n—$.

Key words: copper(II), heterospin complexes, nitroxide biradicals, X-ray diffraction study, magnetic properties.

Specific magnetic anomalies, which are similar in the character of the temperature dependence of the effective magnetic moment (μ_{eff}) to spin transitions, were described for the family of complexes of copper(II) hexafluoroacetylacetonate $Cu(hfac)_2$ (hfac is hexafluoroacetylacetonate) with 1-alkylpyrazol-4-yl-substituted nitronyl nitroxides (L^R).[1—5] In the solid state, these complexes exist as heterospin 1D head-to-head or head-to-tail polymers formed through the bridging coordination of L^R with the involvement of the O atom of one >N—O group and the N atom of the pyrazole ring.

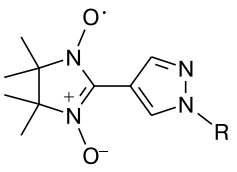

L^R

R = Me, Et, Pr^n, Pr^i, Bu^n

Recently, we have examined the possibility of synthesizing heterospin structures of higher dimensionality (2D and 3D) based on the $Cu(hfac)_2$ complexes with 1-alkylpyrazol-4-yl-substituted nitronyl nitroxides. For this purpose, we used the biradicals L^4 and L^8 containing tetra- and octamethylene binding groups, respectively, between the pyrazole fragments (index *n* in the notation of the biradical L^n corresponds to the number of the methylene units) as building blocks, which can provoke an increase in the dimensionality of the complexes.

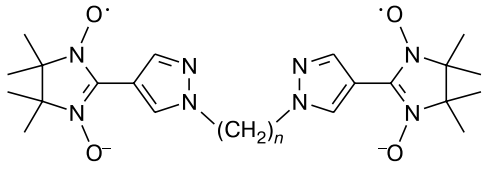

L^n

n = 4, 6, 8, 10, 12

This approach proved to be useful. The reactions of $Cu(hfac)_2$ with L^4 and L^8 were found to produce a complex having a framework structure in the solid state and a layer-polymeric complex, respectively.[6] It appeared that the $—(CH_2)_4—$ and $—(CH_2)_8—$ bridges chosen for the biradicals give rise to rather "rigid" structures compared to 1D complexes. The change scale (Δd) for the Cu—N and Cu—O bond lengths in the coordination units responsible for the possibility of a magnetic anomaly served as the measure of "rigidity".[6] In this connection, we synthesized the complexes of $Cu(hfac)_2$ with the biradicals L^6, L^{10}, and L^{12} and studied the magneto-structural correlations for these complexes in the expectation that the change from L^4 to L^6 and from L^8 to L^{10} (and, the more so, to L^{12}) would lead to a weakening of the rigidity of the structures with increasing number of methylene units in

* Dedicated to Academician G. A. Abakumov on the occasion of his 70th birthday.
† Deceased.

Published in Russian in *Izvestiya Akademii Nauk. Seriya Khimicheskaya,* No. 9, pp. 1732—1741, September, 2007.
1066-5285/07/5609-1795

the bridge. The reactions of $Cu(hfac)_2$ with the biradicals L^6, L^{10}, and L^{12} were found to produce heterospin polymeric complexes. In the solid-state complexes, there are heterospin chains analogous to those found earlier in the $Cu(hfac)_2L^R$ complexes.[1–5] However, the stereochemical nonrigidity observed in the polymeric chains $Cu(hfac)_2L^R$, the framework complex $[Cu(hfac)_2]_2L^6$, and the layer-polymeric complexes $[Cu(hfac)_2]_2L^{10}$ and $\{[Cu(hfac)_2]_2L^{12}\}[Cu(hfac)_2(Pr^iOH)_2]$ is sifted from the coordination units to the polymethylene fragments of the biradicals.

Results and Discussion

Structures and magnetic properties of compounds. The use of biradicals with symmetrical electron-donating groups in the synthesis of complexes does not automatically lead to the self-assembly of heterospin complexes of high dimensionality. For example, the Cambridge Structural Database[7] contains information on the structures of several tens of transition metal complexes with nitronyl nitroxide and imino nitroxide biradicals, among which only a few compounds have a polymeric structure in the solid state.[6,8,9]

To construct structures of high dimensionality, a particular complex of requirements should be met. Even when excluding the kinetic and thermodynamic factors that are difficult to predict and analyzing only the structural complementarity of the building blocks, from which a structure of high dimensionality can, in principle, be assembled, a rather large number of possible combinations still remain to be considered.[10,11] Hence, we carried out the preliminary structural modeling of the possible packings before performing the synthesis of the complexes of $Cu(hfac)_2$ with L^4 and L^8. First, we took into account that the bidentate bridging coordination of the paramagnetic ligand provoking the chain formation is favorable in the overwhelming majority of the complexes of $Cu(hfac)_2$ with the monoradicals L^R synthesized earlier. For the biradical molecules, the choice of n in the $-(CH_2)_n$ group necessary for the cross-linking of these chains was based on the available structural data for chain polymers of $Cu(hfac)_2$ with 1-alkylpyrazol-4-yl-substituted nitronyl nitroxides.[1–4]

The structural modeling showed that strong structural distortions and strains should appear in both head-to-head and head-to-tail polymer chains upon their cross-linking by polymethylene bridges, in which the number of methylene units between the pyrazole fragments is ≤4. At the same time, according to the results of structural modeling, the presence of more then eight methylene units in the $-(CH_2)_n-$ fragment is excessive and can cause their unpredictable twisting. For this reason, we chose derivatives with $n = 4$ and $n = 8$ as biradicals.

The study of the structure of the $[Cu(hfac)_2]_2L^4$ complex showed[6] that nature has solved the problem of strong structural strains for $-(CH_2)_4-$ by creating a framework structure of the heterospin complex with a very high crystal density (1.708 g cm^{-3}) untypical of this class of compounds. The polymethylene fragments $-(CH_2)_8-$ in the polymeric layers of the real $[Cu(hfac)_2]_2L^8$ complex are only slightly contracted, which is in good agreement with the results of preliminary modeling. In the real structure of $[Cu(hfac)_2]_2L^8$, the distance between the N atoms linked by the $-(CH_2)_8-$ fragments is 11.260(8) Å, which is close to the maximum value (11.505 Å) and is substantially larger than the average value (10.81±0.12 Å) for the $-N(CH_2)_8N-$ fragments available in the Cambridge Structural Database.[7] Hence, when designing the present study, we planned to answer the following two main questions: 1) whether the framework structure of the heterospin complex is retained in going from L^4 to L^6 and 2) how the stereochemical nonrigidity of the layered structure is provided in going from L^8 to L^{10} (and the more so to L^{12}).

Since we succeeded in finding answers to both questions, let us turn our attention to the structure of $[Cu(hfac)_2]_2L^6$ (Fig. 1) without a detailed consideration of the synthesis of the biradicals and heterospin complexes. In the crystal structure of this complex, the paramagnetic ligands serve as tetradentate bridges. Each Cu atom is coordinated by two L^6 ligands through the O atom of the >N—O group and the N atom of the pyrazole fragment. Unlike the $[Cu(hfac)_2]_2L^4$ complex studied earlier, in which all nitroxides are coordinated in a head-to-tail fashion (Fig. 1, *d*),[6] the paramagnetic ligands in $[Cu(hfac)_2]_2L^6$ are coordinated in a head-to-head fashion. The structure consists of 66-membered metallocycles (Fig. 1, *a*) that are fused to form a framework. In the simplified form, the scheme of the framework formation is presented in Fig. 1, *b*. One metallocycle can be outlined in this framework (Fig. 1, *c*).

An important structural feature of $[Cu(hfac)_2]_2L^6$ is that the distances between the paramagnetic centers, Cu—O_L, in all CuO_6 coordination units are 2.030(3) Å (Table 1). These short distances (O_{hfac} atoms lie on the elongated axis, $d(Cu—O_{hfac})$ = 2.206(4) Å, see Table 1) are responsible for strong antiferromagnetic exchange interactions in the exchange clusters >N—$^{\bullet}$O—Cu—O$^{\bullet}$—N<. The theoretical simulation of the experimental temperature dependence of the effective magnetic moment (μ_{eff}) (Fig. 2) was carried out with the use of the isotropic spin Hamiltonian ($\hat{H} = -2J\sum \hat{S}_i\hat{S}_j$) and the program for calculations of heterospin exchange clusters.[13] As a result, we obtained the following numerical estimates for the exchange parameters for $[Cu(hfac)_2]_2L^6$: J(>N—$^{\bullet}$O—Cu—O$^{\bullet}$—N<) = −191 cm^{-1} and zJ' = −0.25 cm^{-1}. Therefore, in full agreement with the structural data, the magnetic structure of the complex

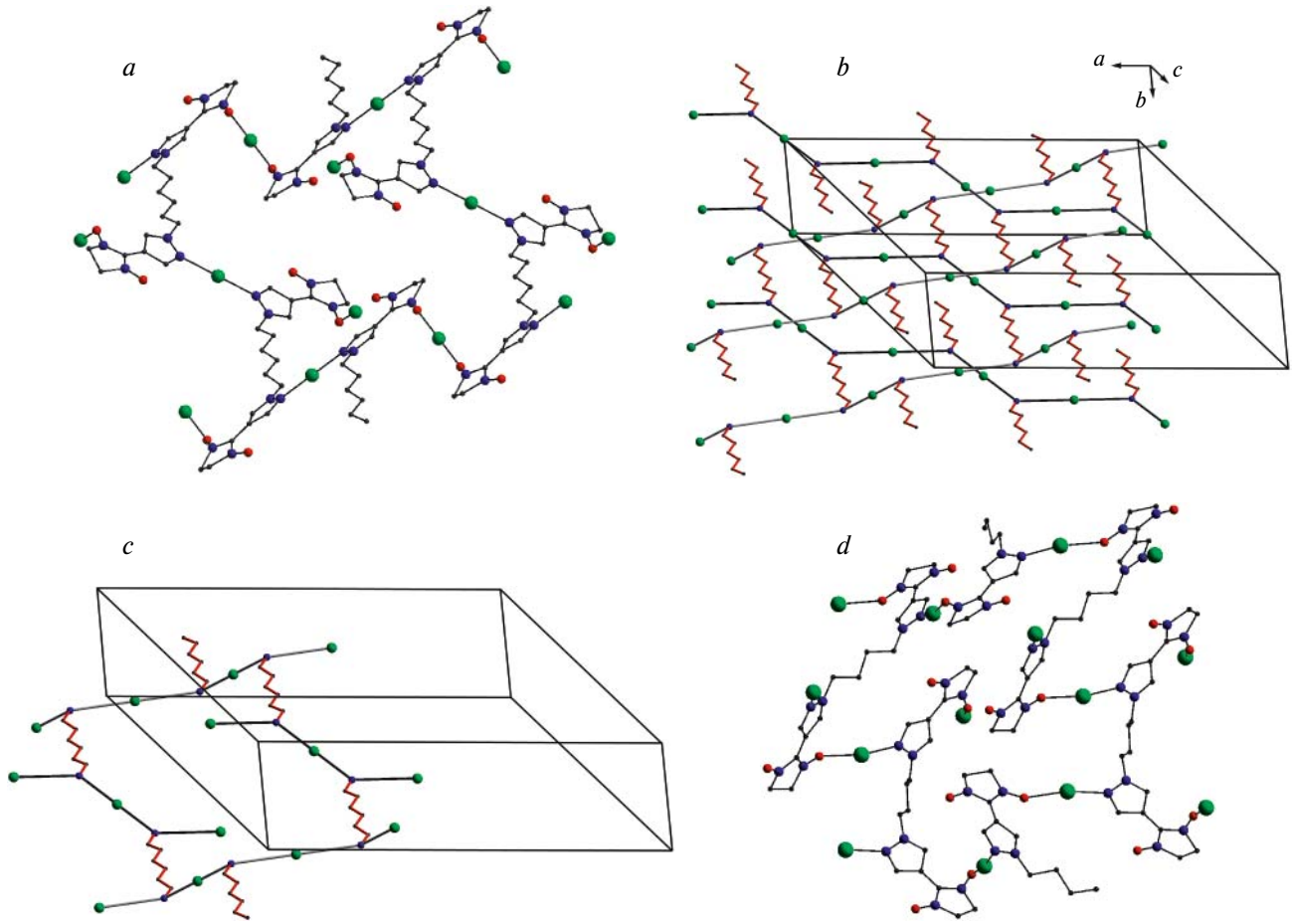

Fig. 1. *a*. Structure of the 66-membered metallocycle in the $[Cu(hfac)_2]_2L^6$ complex; the hfac fragments, the Me groups of the 2-imidazoline ring, and the H atoms are omitted; Cu, O, and N atoms are shown in green, red, and blue, respectively. *b*. The scheme of the framework formation in $[Cu(hfac)_2]_2L^6$. *c*. The metallocycle outlined in the framework structure. *d*. The structure of the 66-membered metallocycle in the $[Cu(hfac)_2]_2L^4$ complex.
Note. Fig. 1 is available in full color in the on-line version of the journal (http://www.springerlink.com/issn/1573-9171/current) and on the web-site of the journal (http://russchembull.ru).

is formed by three-center exchange clusters, which are located in the CuO_6 coordination units and are linked by weak exchange interactions with the quasi-isolated Cu^{II} ions in the CuN_2O_4 units. These interactions were taken into account employing the exchange parameter zJ'.

Therefore, the framework structure of the $[Cu(hfac)_2]_2L^n$ complex in the solid state appeared to be favorable for $n = 4$ and 6. The framework of both $[Cu(hfac)_2]_2L^4$ and $[Cu(hfac)_2]_2L^6$ is formed by the fused 66-membered metallocycles (see Fig. 1, *a*, *c*). An increase in the length of the polymethylene chain in L^6 compared to that in L^4 is compensated by the change from the head-to-tail structure typical of $[Cu(hfac)_2]_2L^4$ within the 66-membered metallocycles to the head-to-head structure in $[Cu(hfac)_2]_2L^6$.

Let us consider the changes in the structure of $[Cu(hfac)_2]_2L^{10}$ compared to $[Cu(hfac)_2]_2L^8$. First, the layer-polymeric structure of the solid phase is retained (Fig. 3, *a*, *b*). Second, as expected, the presence of additional methylene units between the radical fragments reduces the steric strain. It appeared that the $[Cu(hfac)_2]_2L^{10}$ complex can be isolated as two polymorphs, $[Cu(hfac)_2]_2L^{10}$-I and $[Cu(hfac)_2]_2L^{10}$-II, whereas this effect was not observed for $[Cu(hfac)_2]_2L^8$. The difference in the structure of the polymeric layers in these modifications is presented in Fig. 3, *a*, *b*. In Fig. 3, *a*, the chain consisting of Cu atoms and halves of the molecules L^{10} is formally outlined by dash-dotted lines within a fragment of the polymeric layer in $[Cu(hfac)_2]_2L^{10}$-I. In these chains, the monoradical fragments are coordinated exclusively in a head-to-tail fashion. In the $[Cu(hfac)_2]_2L^{10}$-II modification, analogous head-to-tail chains, which are also indicated by dash-dotted lines, alternate with head-to-head chains (see Fig. 3, *b*). For comparison, Fig. 3, *c* shows a fragment of the layer in the $[Cu(hfac)_2]_2L^8$ complex studied earlier,[6] in which all

Table 1. Selected bond lengths (*d*) and bond angles (ω) in the complexes

Compound	*d*/Å					ω/deg		
	Cu—O_L	Cu—O_{hfac}	Cu′—O′$_{hfac}$	Cu—N	N—O	Cu—O_L—N	Im—Pz	Pz—Pz
$[Cu(hfac)_2]_2L^6$	2.030(3)	2.007(3)	1.954(3)	2.454(4)	1.297(4)	124.0(3)	11.6	65.9
		2.206(4)	1.973(3)		1.275(5)			
$[Cu(hfac)_2]_2L^{10}$-I	2.399(6)	1.934(6)	—	2.377(6)	1.284(8)	153.3(7)	10.3	180.0
		1.940(5)			1.272(8)			
		1.936(6)	—					
		1.941(5)						
$[Cu(hfac)_2]_2L^{10}$-II	2.402(5)	1.944(5)	1.983(5)	2.283(6)	1.282(8)	131.7(5)	2.5	22.9
		1.955(5)	2.026(6)		1.255(9)			
	2.516(6)	1.936(6)	1.947(6)	2.390(7)	1.273(7)	142.2(6)	8.7	
		1.942(5)	1.950(5)		1.291(7)			
{$[Cu(hfac)_2]_2L^{12}$-$[Cu(hfac)_2(Pr^iOH)_2]$}	2.423(4)	1.933(4)	1.988(5)	2.312(6)	1.283(6)	127.8(3)	8.1	180.0
		1.933(4)	2.010(5)					
	2.360(7)*	1.907(5)			1.266(6)			
		1.972(6)						
$[Cu(hfac)_2]_4L^8$	1.932(3)	1.943(3)	1.956(3)	2.320(3)	1.319(4)	119.7(2)	10.0	180.0
		1.975(3)	1.963(3)					
		1.972(3)	1.958(2)		1.283(5)			
		2.183(3)	1.977(3)					
$[Cu(hfac)_2]_4L^{10}\cdot C_6H_{14}$	1.928(4)	1.908(5)	1.932(4)	1.999(4)	1.298(6)	120.7(3)	10.0	180.0
		1.940(5)	1.978(4)					
		1.930(5)	1.932(4)		1.261(6)			
		2.194(4)	2.121(4)					

* Cu—O_{ROH}.

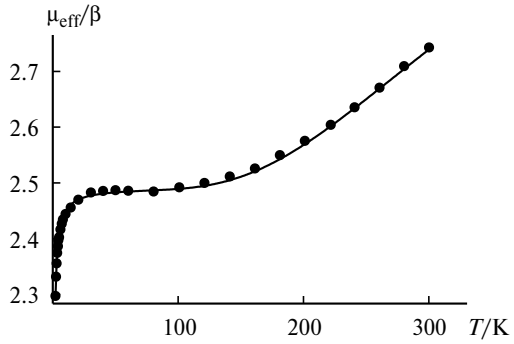

Fig. 2. Dependence $\mu_{eff}(T)$ for the $[Cu(hfac)_2]_2L^6$ complex; points correspond to the experimental data; the solid curve, to the calculated data.

analogous chains are arranged in a head-to-head fashion. This type of the layer formation proved to be optimal for the "rigid" structure of $[Cu(hfac)_2]_2L^8$. However, the "rigidity" of the structure is not evident from Fig. 3, *a*—*c*, where the arrangements of the layers are presented. Since the nitronyl nitroxide fragments together with the pyrazole rings and the $\{Cu(hfac)_2\}_2$ fragments are structurally similar in $[Cu(hfac)_2]_2L^8$, $[Cu(hfac)_2]_2L^{10}$-I, and $[Cu(hfac)_2]_2L^{10}$-II, it is reasonable to compare the structures of the polymetylene units in the real structures. In the solid state of $[Cu(hfac)_2]_2L^8$, the octamethylene system $—(CH_2)_8—$ has a zigzag structure (see Fig. 3, *d*). In the $Cu(hfac)_2]_2L^{10}$-I and $[Cu(hfac)_2]_2L^{10}$-II modifications containing a larger number of methylene units, the decamethylene system $—(CH_2)_{10}—$ is either twisted to form a helix or is bent as a spring in the effort to form a close packing. These data show that the $—(CH_2)_{10}—$ fragments, which are twisted in one or another fashion, are most prone to structural variations in the crystals of $[Cu(hfac)_2]_2L^{10}$-I and $[Cu(hfac)_2]_2L^{10}$-II. This is the main difference between the layered heterospin systems $[Cu(hfac)_2]_2L^{10}$-I and $[Cu(hfac)_2]_2L^{10}$-II, on the one hand, and the chain polymers $Cu(hfac)_2L^R$ arranged in a head-to-head or head-to-tail fashion, which have been studied earlier, on the other hand.[1—4] In the structure of $Cu(hfac)_2L^R$, the coordination units serve as stereochemically nonrigid parts, whereas the nonrigidity is shifted to the polymethylene fragments in layer-polymeric systems.

The large distances between the Cu atom and the O atom in the nitroxide ligands (Cu—O_L, see Table 1) in $[Cu(hfac)_2]_2L^{10}$-I and $[Cu(hfac)_2]_2L^{10}$-II (2.399(6), 2.402(5), and 2.516(6) Å) correlate with the ferromagnetic character of exchange interactions in the exchange clusters Cu—O$^\bullet$—N< and >N—$^\bullet$O—Cu—O$^\bullet$—N<. The magnetic structure of $[Cu(hfac)_2]_2L^{10}$-I can be represented as consisting of the exchange clusters Cu—O$^\bullet$—N< (exchange parameter J) linked to each other by the exchange interactions J_1. In this approximation, the experi-

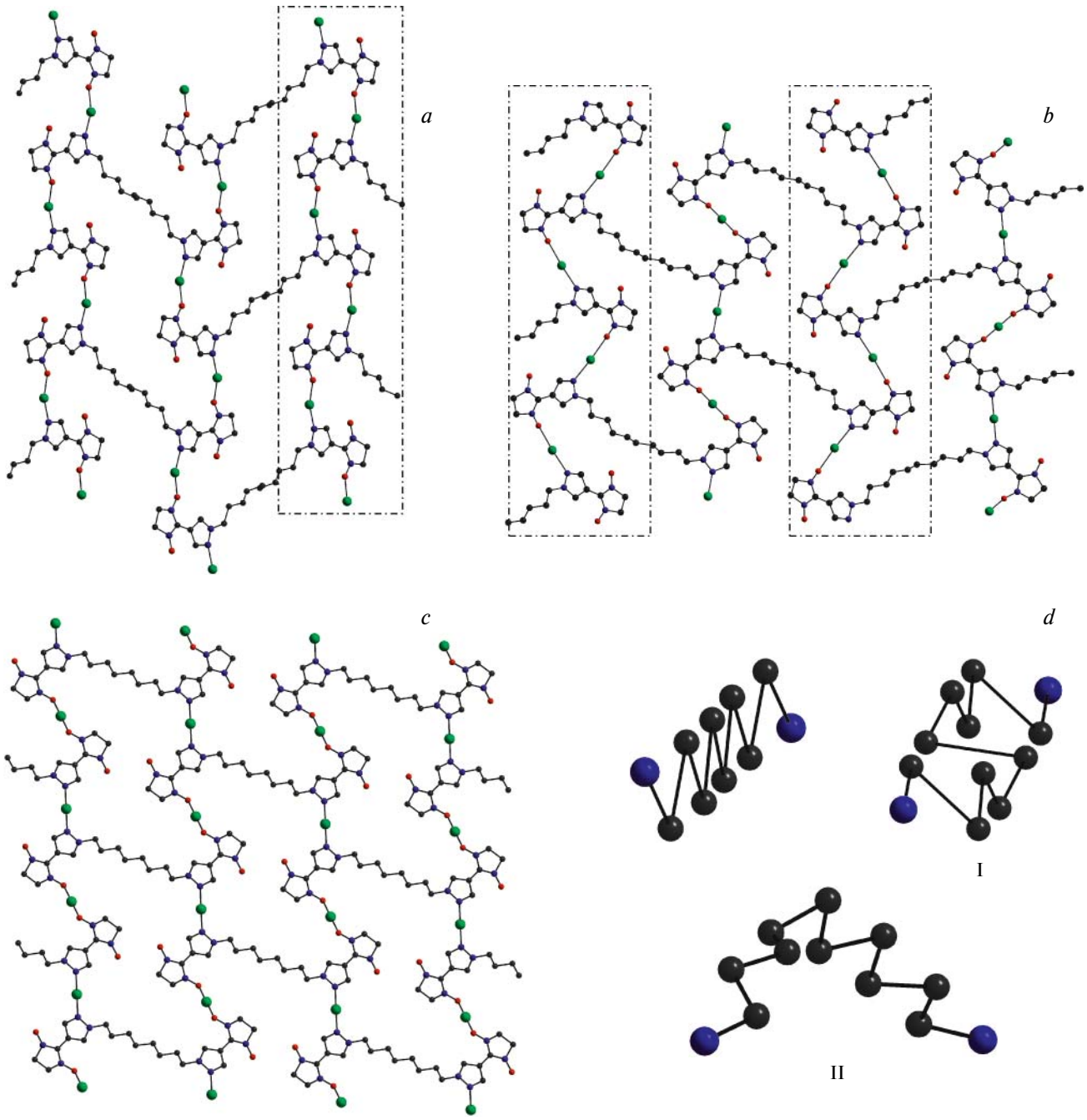

Fig. 3. Structure of the layers in the crystals of $[Cu(hfac)_2]_2L^{10}$-I (*a*), $[Cu(hfac)_2]_2L^{10}$-II (*b*), and $[Cu(hfac)_2]_2L^{8}$ (*c*). Head-to-tail chains are indicated by dash-dotted lines. The hfac fragments, the Me groups of the 2-imidazoline ring, and the hydrogen atoms are omitted; Cu, O, and N atoms are shown in green, red, and blue, respectively. *d*. The N—$(CH_2)_n$—N fragments in the $[Cu(hfac)_2]_2L^{8}$, $[Cu(hfac)_2]_2L^{10}$-I, and $[Cu(hfac)_2]_2L^{10}$-II complexes.
Note. Fig. 3 is available in full color in the on-line version of the journal (http://www.springerlink.com/issn/1573-9171/current) and on the web-site of the journal (http://russchembull.ru).

mental dependence $\mu_{eff}(T)$ for the $[Cu(hfac)_2]_2L^{10}$-I complex (Fig. 4) is described by the following optimal exchange parameters: $J = 7.2$ cm^{-1}, $J_1 \approx 0$ cm^{-1}, and $zJ' = -0.042$ cm^{-1}. The magnetic structure of $[Cu(hfac)_2]_2L^{10}$-II is formed by the exchange clusters Cu—O$^{\bullet}$—N< (exchange parameter J_1), the exchange clusters >N—$^{\bullet}$O—Cu—O$^{\bullet}$—N< (J_2), and the quasi-isolated Cu^{II} ions. For this complex, the theoretical curve corresponds to the following optimal exchange parameters: $J_1 = 33$ cm^{-1}, $J_2 = 14$ cm^{-1}, and $zJ' = -0.04$ cm^{-1}.

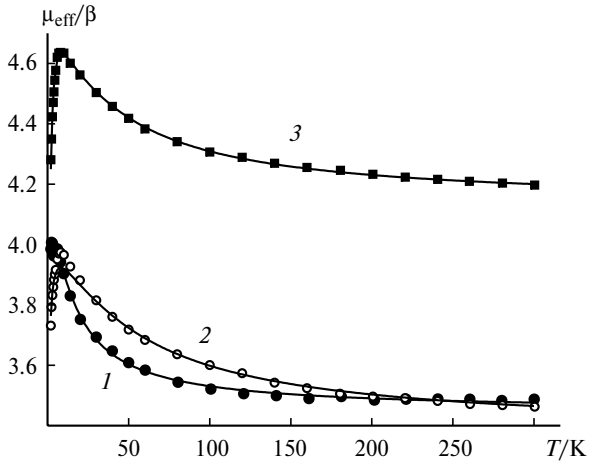

Fig. 4. Temperature dependences of the effective magnetic moment for $[Cu(hfac)_2]_2L^{10}$-I (*1*), $[Cu(hfac)_2]_2L^{10}$-II (*2*), and $\{[Cu(hfac)_2]_2L^{12}\}[Cu(hfac)_2(Pr^iOH)_2]$ (*3*); points correspond to the experimental data; the solid curves, to the calculated data.

It should be noted that the high-temperature asymptotics of μ_{eff} for both $[Cu(hfac)_2]_2L^{10}$-I and $[Cu(hfac)_2]_2L^{10}$-II tends to 3.46 β, which is theoretically estimated for the sum of the contributions made by four weakly interacting paramagnetic centers with $s = 1/2$ and $g = 2.0$ to the magnetic susceptibility.

The twisting and bending of the polymethylene chain is observed also in the structure of the complex with the biradical L^{12} (Fig. 5, *b*). The structure of $\{[Cu(hfac)_2]_2L^{12}\}[Cu(hfac)_2(Pr^iOH)_2]$ is also formed by polymeric layers, in which head-to-head chains can formally be distinguished (Fig. 5, *a*). However, when the number of the polymethylene units is increased to 12, the cavities in the layers become so large that they can be occupied by molecules of the $Cu(hfac)_2$ complexes with coordinated isopropyl alcohol (Fig. 5, *a*), which was used for the crystal growth. In this case, the Pr^iOH molecules are additionally bound to the polymeric layers by hydrogen bonds between the OH groups of the coordinated alcohol molecules and the N—O groups of the nitronyl nitroxide fragments ($O_{Pr^iOH}...O_L$, 2.769(8) Å). A comparison of the structures of the layers in $[Cu(hfac)_2]_2L^8$, $[Cu(hfac)_2]_2L^{10}$-I, and $[Cu(hfac)_2]_2L^{10}$-II with the structure of the layer in $\{[Cu(hfac)_2]_2L^{12}\}[Cu(hfac)_2(Pr^iOH)_2]$ presents difficulties due to the presence of the additional $Cu(hfac)_2$ matrix in the latter structure. However, the structure of the $N—(CH_2)_{12}—N$ fragments in the crystal structure of the latter complex (Fig. 5, *b*) provides evidence that they are prone to twisting and bending, *i.e.*, serve as springs compensating possible strains in the polymeric layer.

The magnetic properties of the heterospin complex $\{[Cu(hfac)_2]_2L^{12}\}[Cu(hfac)_2(Pr^iOH)_2]$ are similar to those of the $[Cu(hfac)_2]_2L^{10}$-I and $[Cu(hfac)_2]_2L^{10}$-II modifications (see Fig. 4). The presence of the

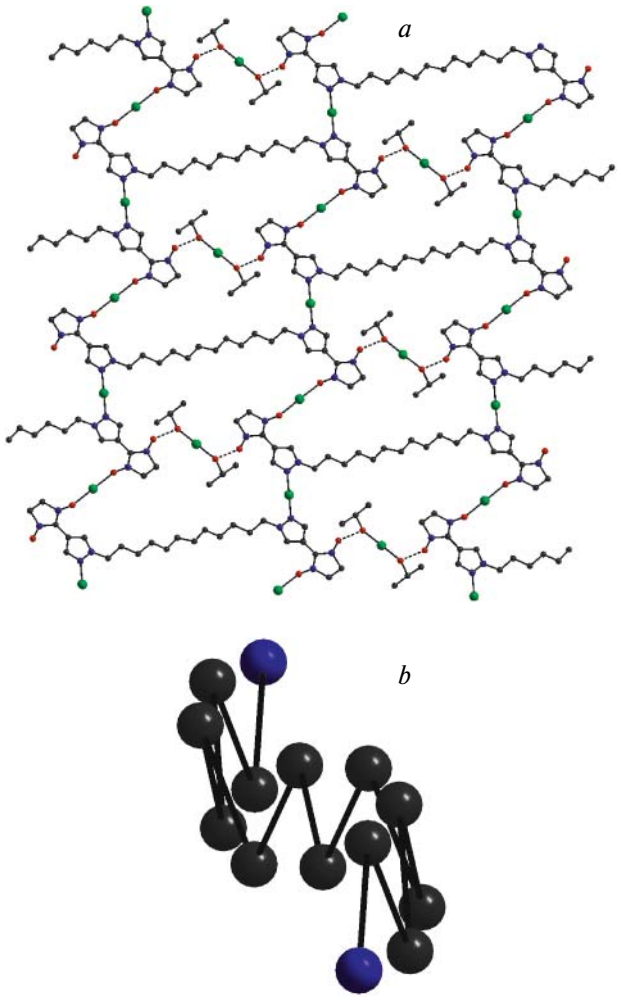

Fig. 5. Structures of the layer (*a*) and the $N—(CH_2)_{12}—N$ fragment (*b*) in the $\{[Cu(hfac)_2]_2L^{12}\}[Cu(hfac)_2(Pr^iOH)_2]$ complex. *Note.* Fig. 5 is available in full color in the on-line version of the journal (http://www.springerlink.com/issn/1573-9171/current) and on the web-site of the journal (http://russchembull.ru).

additional bis-chelate $Cu(hfac)_2$ matrix in the $\{[Cu(hfac)_2]_2L^{12}\}[Cu(hfac)_2(Pr^iOH)_2]$ complex and, correspondingly, the larger number of paramagnetic centers compared to those in the complexes with L^{10} are responsible for the larger effective magnetic moments. In the structure of $\{[Cu(hfac)_2]_2L^{12}\}_2[Cu(hfac)_2(Pr^iOH)_2]$, there are two essential channels of exchange interactions between the paramagnetic centers: the direct exchange interaction $Cu^{II}—O^{\bullet}—N<$ (J_1) and the exchange interaction between Cu^{II} and the nitroxide groups through the OH group of the coordinated alcohol molecule (J_2). The energies of interactions through other channels are small and they were taken into account in the optimization with the use of the exchange parameter zJ'. The theoretical curve in Fig. 4 corresponds to the following optimal parameters: $J_1 = 29$ cm^{-1}, $J_2 = 9.4$ cm^{-1}, and $zJ' = -0.16$ cm^{-1}.

The formation of layer-polymeric compounds can be suppressed by the addition of an excessive amount of $Cu(hfac)_2$ to the reaction system. For example, the molecular complexes $[Cu(hfac)_2]_4L^8$ and $[Cu(hfac)_2]_4L^{10}$ were synthesized by the reactions with the ligands L^8 and L^{10}, respectively, using the $Cu(hfac)_2$/biradical stoichiometric ratio of 4/1. The molecules of these complexes are centrosymmetric with respect to the midpoint of the polymetylene bridge and have similar structures (Fig. 6). The coordination environment of the Cu atoms can be described as a distorted square pyramid, except for the $CuNO_4$ units in $[Cu(hfac)_2]_4L^{10}$, in which the coordination environment of the Cu^{II} atoms is better described by a trigonal bipyramid. The most important feature of their structures is the presence of short equatorial distances between the Cu atoms and the O atoms of the coordinated nitroxide groups (1.932(3) Å in $[Cu(hfac)_2]_4L^8$ and 1.928(4) Å in $[Cu(hfac)_2]_4L^{10}$), which is responsible for very strong antiferromagnetic exchange interactions between the unpaired electrons of the Cu^{II} atoms and the coordinated nitroxide groups in the CuO_5 units. As a result, the spins in the exchange clusters Cu—O•—N< are virtually fully paired already at room temperature, and the contributions to the residual effective magnetic moment are made primarily by the isolated Cu^{II} atoms of the $CuNO_4$ coordination units. Since these units are substantially spaced from each other, the interactions between these units are weak, and the magnetic moment μ_{eff} remains almost unchanged with temperature: μ_{eff} is 3.05 and 2.86 β at 300 and 2 K, respectively, for $Cu(hfac)_2]_4L^8$; μ_{eff} is 3.05 and 2.95 β at 300 and 2 K, respectively, for $[Cu(hfac)_2]_4L^{10}$.

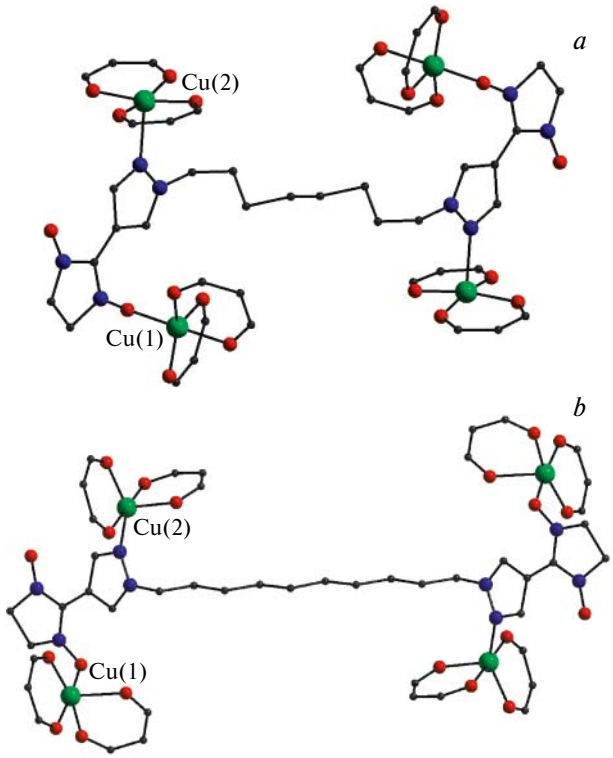

Fig. 6. Molecular structures of $[Cu(hfac)_2]_4L^8$ (*a*) and $[Cu(hfac)_2]_4L^{10}$ (*b*); the CF_3 and CH_3 groups and the H atoms are omitted; Cu, O, and N atoms are shown in green, red, and blue, respectively.

Note. Fig. 6 is available in full color in the on-line version of the journal (http://www.springerlink.com/issn/1573-9171/current) and on the web-site of the journal (http://russchembull.ru).

Synthesis of biradicals and complexes. The possibility of alkylation of L^H and the procedure developed for the synthesis of this compound[12] allow the preparation of L^n with the desired number of methylene units. The alkylation of L^H with 1,6-dibromohexane, 1,10-dibromodecane, or 1,12-dibromododecane under phase-transfer catalysis (Scheme 2) produced nitroxides L^6, L^{10}, and L^{12}, respectively, in ~40—50% yields. In addition, nitroxide L^{12} was prepared by the independent synthesis based on the introduction of the polymethylene group in early steps (Scheme 1).

Scheme 1

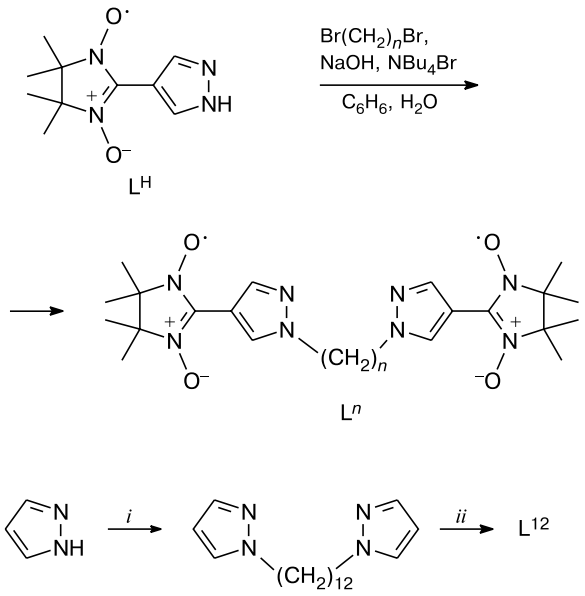

DHA is 2,3-di(hydroxyamino)-2,3-dimethylbutane

i. $Br(CH_2)_{12}Br$, NaOH, $BuNHSO_4$, H_2O.
ii. 1) $POCl_3$, DMF, 2) DHA, MeOH, 3) $NaIO_4$, H_2O, $CHCl_3$

Weak antiferromagnetic exchange interactions are present in the solid state of the biradicals L^6, L^{10}, and L^{12}. The temperature dependences of the effective magnetic moment for the biradicals L^6, L^{10}, and L^{12} are similar; the typical curve is exemplified by L^{12} in Fig. 7.

The heterospin complexes $[Cu(hfac)_2]_2L^n$ were synthesized by the reactions of $[Cu(hfac)_2]$ with the corresponding L^n. It is difficult to grow single crystals of these

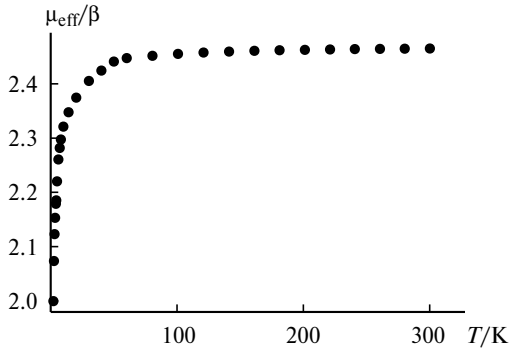

Fig. 7. Dependence $\mu_{eff}(T)$ for L^{12}.

compounds suitable for X-ray diffraction because of their high solubility in low-polarity organic solvents. In addition, the storage of concentrated solutions for 12 h or a longer period of time led to a gradual accumulation of decomposition products in these solutions, which substantially hindered the crystallization of the target products. As a rule, the use of an acetone—heptane (or hexane) mixture resulted in the formation of oily products. The subsequent addition of a diethyl ether—hexane mixture or pure hexane to the oily residue resulted in the fast crystallization of $[Cu(hfac)_2]_2L^{10}$-I and $[Cu(hfac)_2]_2L^{10}$-II, respectively. It should be noted that $[Cu(hfac)_2]_2L^{10}$-II crystallizes also from solutions in diethyl ether containing equimolar amounts of L^{10} and $[Cu(hfac)_2]_4L^{10}$. The latter, in turn, is readily formed upon the dissolution of the oily or finely crystalline $[Cu(hfac)_2]_2L^{10}$ complex in hexane followed by the addition of two equivalents of $Cu(hfac)_2$. Ethanol proved to be the solvent of choice for $[Cu(hfac)_2]_2L^6$, which is the least soluble compound among the complexes under consideration.

To summarize, we synthesized the framework heterospin complex ($[Cu(hfac)_2]_2L^6$) and the layer-polymeric heterospin complexes ($[Cu(hfac)_2]_2L^{10}$ and $\{[Cu(hfac)_2]_2L^{12}\}[Cu(hfac)_2(Pr^iOH)_2]$). Since the stereochemical nonrigidity in the solid state of these compounds is manifested as a deformation of the polymethylene fragments, no anomalies in the curves $\mu_{eff}(T)$ were found, as opposed to the chain-polymeric complexes $[Cu(hfac)_2]L^R$ studied earlier.[1—4]

Experimental

General methods. The progress of the reactions was monitored by TLC on Silica gel 60 F_{254} aluminum sheets (Merck). The solvents were removed from the reaction mixtures under reduced pressure at 30—35 °C on a rotary evaporator. The column chromatography was performed on silica gel (0.063—0.200 mm, Merck) and Al_2O_3 (high-purity grade, Donetsk Plant of Chemical Reagents, Ukraine). The IR spectra were recorded in the 400—4000 cm^{-1} region (KBr pellets) on a Bruker Vector-22 spectrophotometer. The melting points were determined on a Boetius hot-stage apparatus. The microanalyses were carried out on a Carlo-Erba 1106 analyzer at the N. N. Vorozhtsov Novosibirsk Institute of Organic Chemistry of the Siberian Branch of the Russian Academy of Sciences. The magnetic susceptibility (χ) was measured on a SQUID MPMS-5S Quantum Design magnetometer in the temperature range of 2—300 K at a magnetic field strength of 5 kOe. The paramagnetic components of the magnetic susceptibility were calculated taking into account the diamagnetic contribution estimated from the Pascal constants. The effective magnetic moment was calculated by the equation

$$\mu_{eff} = [3k\chi T/(N_A\beta^2)]^{1/2},$$

where N_A is Avogadro's number, β is the Bohr magneton, and k is the Boltzmann constant.

1,12-Di(1*H*-pyrazol-1-yl)dodecane (1). 1*H*-Pyrazole (3.4 g, 50 mmol) was added to a solution of KOH (10 g, 0.18 mol) in water (30 mL). The reaction mixture was stirred at room temperature for 15 min. Then 1,12-dibromododecane (8.2 g, 25 mmol) and $(Bu_4N)HSO_4$ (1.7 g, 5 mmol) were added, and the reaction mixture was stirred at 100 °C for 24 h. In the course of the reaction, a white crystalline compound formed on the surface of the aqueous phase. After cooling, the aqueous phase was decanted, the residue was dissolved in CH_2Cl_2 and dried over Na_2SO_4, and the solvent was distilled off. The residue was recrystallized from a mixture of CH_2Cl_2 and hexane. The yield was 6.8 g (90%), m.p. 64—66 °C. Found (%): C, 71.6; H, 10.1; N, 18.5. $C_{18}H_{30}N_4$. Calculated (%): C, 71.5; H, 10.0; N, 18.5. IR, ν/cm^{-1}: 460, 621, 661, 724, 752, 878, 920, 969, 1044, 1092, 1115, 1199, 1283, 1376, 1396, 1468, 1512, 1627, 2847, 2918, 3116, 3434.

1,6-Di[4-(4,4,5,5-tetramethyl-3-oxide-1-oxyl-4,5-dihydro-1*H*-imidazol-2-yl)-1*H*-pyrazol-1-yl]hexane (L^6). A mixture of L^H (0.32 g, 1.4 mmol), 1,6-dibromohexane (0.18 g, 0.7 mmol), $(Bu_4N)Br$ (0.038 g, 0.12 mmol), NaOH (0.058 g, 1.5 mmol), C_6H_6 (3.6 mL), and H_2O (2.2 mL) was stirred at 50 °C for 72 h. Then the reaction mixture was cooled, the organic layer was separated, and the aqueous phase was extracted with $CHCl_3$ (4×5 mL). The organic phases were combined and dried with Na_2SO_4. The solvents were distilled off, and the oily residue was purified by chromatography on a 2.5×20 cm alumina column using ethyl acetate as the eluent. The blue fraction containing a compound with $R_f = 0.5$ was collected and concentrated. The residue was purified on a 1.5×25 cm silica gel column using ethyl acetate as the eluent. The blue fraction containing the reaction product was eluted last. This fraction was concentrated, and the oily residue was dissolved in an Et_2O—hexane mixture. The solution was kept in an open flask at 0 °C. Small dark-blue crystals that formed were filtered off and dried in air. The yield was 0.19 g (51%), m.p. 179—182 °C. Found (%): C, 59.1; H, 7.6; N, 21.2. $C_{26}H_{40}N_8O_4$. Calculated (%): C, 58.6; H, 7.8; N, 20.7. IR, ν/cm^{-1}: 419, 462, 540, 647, 666, 753, 812, 869, 906, 981, 1013, 1050, 1130, 1181, 1216, 1308, 1322, 1358, 1371, 1401, 1423, 1445, 1598, 2859, 2930, 2958, 2992, 3140, 3421.

1,10-Di[4-(4,4,5,5-tetramethyl-3-oxide-1-oxyl-4,5-dihydro-1*H*-imidazol-2-yl)-1*H*-pyrazol-1-yl]decane (L^{10}) was synthesized analogously to L^6 in 49% yield. M.p. 99—101 °C. Found (%): C, 61.7; H, 8.4; N, 18.9. $C_{30}H_{48}N_8O_4$. Calculated (%): C, 61.6; H, 8.3; N, 19.2. IR, ν/cm^{-1}: 421, 463,

541, 600, 646, 665, 722, 763, 815, 855, 979, 1017, 1129, 1182, 1218, 1322, 1360, 1403, 1423, 1463, 1600, 2849, 2925, 2984, 3127, 3458.

1,12-Di[4-(4,4,5,5-tetramethyl-3-oxide-1-oxyl-4,5-dihydro-1*H*-imidazol-2-yl)-1*H*-pyrazol-1-yl]dodecane (L^{12}). *Method A.* The biradical L^{12} was synthesized analogously to L^6 in 42% yield.

Method B. A mixture of 1,12-di(1*H*-pyrazol-1-yl)dodecane (6 g, 20 mmol) and DMF (9 mL) was heated to 70 °C. Then a solution of $POCl_3$ (6.1 g, 3.7 mL, 40 mmol) in DMF (15.5 mL) was added dropwise with stirring. After 4 h, an additional amount of $POCl_3$ (3.6 g, 2.2 mL, 24 mmol) was added. The reaction mixture was stirred at 70 °C for 30 min and cooled, H_2O (15 mL) was added, and the mixture was neutralized with K_2CO_3 to pH 9—10 and kept in refrigerator for 1 h. The brown solid organic phase that formed was filtered off and dissolved in CH_2Cl_2. The solution was filtered through a layer of Al_2O_3 (2×15 cm) and a layer of SiO_2 (2×15 cm) using CH_2Cl_2 as the eluent. The solvent was distilled off, and the yellow product was recrystallized from a mixture of CH_2Cl_2 and hexane. 1,1′-(Dodecane-1,12-diyl)bis(1*H*-pyrazole-4-carbaldehyde) was obtained in a yield of 3.48 g (49%). The dialdehyde was dissolved in MeOH (50 mL). 2,3-Di(hydroxyamino)-2,3-dimethylbutane (DHA) (2.87 g, 19.4 mmol) was added to the solution. The resulting suspension was stirred for 1.5 h, after which a pale-yellow solution was obtained. The solution was kept at 5 °C for 12 h. The pale-yellow precipitate that formed was filtered off and washed on a filter with cold MeOH. The yield of 2,2′-[1,1′-(dodecane-1,12-diyl)bis(1*H*-pyrazole-4,1-diyl)]bis(4,4,5,5-tetramethylimidazolidine-1,3-diol) was 3.79 g (63%). Then $NaIO_4$ (1.24 g, 5.8 mmol) was added portionwise with stirring to a mixture of imidazolidine-1,3-diol (2 g, 3.2 mmol), CH_2Cl_2 (50 mL), and H_2O (10 mL) at room temperature for 1 h, after which the organic phase turned intense blue. The organic layer was separated, and the aqueous phase was extracted with chloroform (1×10 mL). The combined organic solutions were dried with Na_2SO_4, and the solvent was evaporated. The residue was dissolved in C_6H_6, and the solution was applied on a 2.5×50 cm silica gel column. The product was eluted with ethyl acetate, and the second blue fraction was collected. This fraction was concentrated, and the residue was crystallized by triturating with hexane. The yield was 1.0 g (50%), m.p. 85—87 °C. Found (%): C, 62.9; H, 8.6; N, 18.0. $C_{32}H_{52}N_8O_4$. Calculated (%): C, 62.7; H, 8.6; N, 18.3. IR, ν/cm^{-1}: 412, 462, 485, 541, 598, 642, 666, 718, 761, 814, 830, 867, 980, 1017, 1075, 1130, 1182, 1221, 1307, 1323, 1335, 1359, 1404, 1425, 1465, 1600, 2852, 2924, 2980, 3138, 3444.

Complex $[Cu(hfac)_2]_2L^6$. A mixture of $Cu(hfac)_2$ (181 mg, 0.38 mmol) and L^6 (100 mg, 0.19 mmol) was dissolved in ethanol (3 mL) and kept in an open flask for one day. Large plate-like crystals that formed were filtered off, washed with cold diethyl ether, and dried in air. The yield was 31%. Found (%): C, 37.7; H, 3.2; F, 30.6; N, 7.6. $C_{46}H_{44}F_{24}Cu_2N_8O_{12}$. Calculated (%): C, 37.2; H, 3.0; F, 30.7; N, 7.6.

Complex $[Cu(hfac)_2]_2L^{10}$-I. A mixture of $Cu(hfac)_2$ (327 mg, 0.68 mmol) and L^{10} (200 mg, 0.34 mmol) was dissolved in acetone (2 mL), and the solvent was removed under an air stream until a brown oil formed. The oil was dissolved in diethyl ether (3 mL). Hexane (2 mL) was added to the blue-green solution. After 3 h, blue plate-like crystals that formed were filtered off, washed with a cold diethyl ether—hexane mixture, and dried in air. The yield was 55%. Found (%): C, 39.6; H, 3.3; F, 29.2;

Table 2. Crystallographic characteristics of the complexes and the X-ray data collection and refinement statistics

Parameter	$[Cu(hfac)_2]_2L^6$	$[Cu(hfac)_2]_2L^{10}$-I	$[Cu(hfac)_2]_2L^{10}$-II	$\{[Cu(hfac)_2]_2L^{12}$ $[Cu(hfac)_2(Pr^iOH)_2]\}$	$[Cu(hfac)_2]_4L^8$	$[Cu(hfac)_2]_4L^{10}\cdot$ $\cdot C_6H_{14}$
FW	1483.98	1540.08	1540.08	2165.97	2467.34	2581.52
Space group	*C*2/*c*	$P2_1/n$	*C*2/*c*	$P\bar{1}$	$P\bar{1}$	$P2_1/c$
Z	8	4	8	1	1	2
a/Å	30.399(9)	14.899(6)	25.369(6)	11.5758(17)	9.6643(19)	13.5888(14)
b/Å	9.695(3)	15.565(6)	15.975(3)	15.187(2)	14.998(3)	12.6981(14)
c/Å	24.918(7)	15.638(6)	37.872(8)	15.249(2)	18.471(4)	30.379(3)
α/deg				116.619(3)	102.76(3)	
β/deg	125.895(4)	115.357(7)	101.898(5)	93.081(3)	102.86(3)	93.765(2)
γ/deg				101.155(3)	92.07(3)	
V/Å^3	5949(3)	3277(2)	15019(6)	2321.1(6)	2535.5(9)	5230.7(10)
d_{calc}/g cm^{-3}	1.657	1.561	1.362	1.550	1.616	1.639
μ(Mo-Kα)/mm^{-1}	0.854	0.778	0.679	0.817	0.979	0.953
θ/deg	1.70—23.31	1.58—23.36	1.78—23.41	1.82—23.31	1.16—23.40	2.08—23.29
I_{hkl}*	22133/4291	25039/4745	57322/10831	18027/6650	10972/7222	34355/7510
R_{int}	0.0652	0.1678	0.1765	0.1477	0.0784	0.1281
N	588	527	919	699	784	802
GOOF	1.033	1.065	0.759	0.896	0.950	0.741
R_1	0.0532	0.0918	0.0770	0.0719	0.0457	0.0582
wR_2 ($I > 2\sigma_I$)	0.1448	0.2080	0.1968	0.1569	0.0995	0.1373
R_1	0.0697	0.1464	0.1720	0.1358	0.1608	0.1286
wR_2 (based on all data)	0.1562	0.2396	0.2508	0.1831	0.1521	0.1675

* The number of measured/independent reflections.

N, 7.4. $C_{50}H_{52}F_{24}Cu_2N_8O_{12}$. Calculated (%): C, 39.0; H, 3.4; F, 29.6; N, 7.3.

Complex $[Cu(hfac)_2]_2L^{10}$-II. *Method A.* A mixture of $Cu(hfac)_2$ (163 mg, 0.34 mmol) and L^{10} (100 mg, 0.17 mmol) was dissolved in acetone (2 mL), and the solvent was removed under an air stream until a brown oil formed. Then hexane (2 mL) was added. After 1 h, the blue needle-like crystals that formed were filtered off, washed with hexane, and dried in air. The yield was 91%. Found (%): C, 39.0; H, 3.2; F, 30.5; N, 7.2. $C_{50}H_{52}F_{24}Cu_2N_8O_{12}$. Calculated (%): C, 39.0; H, 3.4; F, 29.6; N, 7.3.

Method B. A mixture of $[Cu(hfac)_2]_4L^{10}$ (200 mg, 0.08 mmol) and L^{10} (47 mg, 0.08 mmol) was dissolved in diethyl ether (5 mL) and kept in an open flask for 2 h. The crystals that formed were filtered off, washed with cold hexane, and dried in air. The yield was 57%. Found (%): C, 39.7; H, 3.5; F, 28.9; N, 7.1. $C_{50}H_{52}F_{24}Cu_2N_8O_{12}$. Calculated (%): C, 39.0; H, 3.4; F, 29.6; N, 7.3.

Complex $[Cu(hfac)_2]_4L^8$. A mixture of $Cu(hfac)_2$ (85.8 mg, 0.18 mmol) and L^8 (25 mg, 0.045 mmol) was dissolved in hexane (3 mL) at 50 °C, and the solution was cooled to room temperature. The brown crystals that formed were filtered off, washed with cold hexane, and dried in air. The yield was 42%. Found (%): C, 33.4; H, 2.2; F, 36.7; N, 4.5. $C_{68}H_{52}F_{48}Cu_4N_8O_{20}$. Calculated (%): C, 33.1; H, 2.1; F, 37.0; N, 4.5.

Complex $[Cu(hfac)_2]_4L^{10}\cdot C_6H_{14}$. A mixture of $[Cu(hfac)_2]_2L^{10}$ (200 mg, 0.13 mmol) and $Cu(hfac)_2$ (124 mg, 0.26 mmol) was dissolved in hexane (25 mL), and the reaction mixture was kept at −18 °C for one day. The brown crystals that formed were filtered off, washed with cold hexane, and dried in air. The yield was 73%. Found (%): C, 36.0; H, 3.0; F, 36.0; N, 4.3. $C_{76}H_{70}F_{48}Cu_4N_8O_{20}$. Calculated (%): C, 35.4; H, 2.7; F, 35.3; N, 4.3.

Complex $\{[Cu(hfac)_2]_2L^{12}\}[Cu(hfac)_2(Pr^iOH)_2]$. A mixture of $Cu(hfac)_2$ (312 mg, 0.65 mmol) and L^{12} (200 mg, 0.33 mmol) was dissolved in isopropyl alcohol (5 mL), and the reaction mixture was kept at −18 °C for one day. The dark-blue crystals that formed were filtered off, washed with cold isopropyl alcohol, and dried in air. The yield was 24%. Found (%): C, 37.8; H, 3.4; F, 31.1; N, 5.2. $C_{68}H_{74}F_{36}Cu_3N_8O_{18}$. Calculated (%): C, 37.7; H, 3.4; F, 31.6; N, 5.2.

X-ray diffraction study. X-ray diffraction data sets were collected from single crystals on a SMART APEX CCD diffractometer (Bruker AXS) (Mo-Kα, λ = 0.71073 Å, T = 295 K). Absorption corrections were applied using the Bruker SADABS software (version 2.10). The structures were solved by direct methods and refined by the full-matrix least-squares method with anisotropic displacement parameters for all nonhydrogen atoms. The positions of some H atoms were located in difference electron density maps. The other H atoms were positioned geometrically. The H atoms of the methyl groups were refined isotropically in the rigid-body approximation. All calculations associated with the structure solution and refinement were carried out with the use of the *Bruker SHELXTL Version 6.14* program package. Selected bond lengths and bond angles are listed in Table 1. The crystallographic characteristics and the X-ray data collection and refinement statistics for the complexes are given in Table 2.

This study was financially supported by the Russian Foundation for Basic Research (Project Nos 05-03-32305, 06-03-32157, 06-03-32742, and 06-03-04000), the US Civilian Research and Development Foundation (CRDF, Grant Y1-C-08-03), the Council on Grants of the President of the Russian Federation (Program for State Support of Leading Scientific Schools of the Russian Federation, Grant NSh-4821.2006.3, and the Program for State Support of Young Scientists, Grant MK-10264.2006.3), and the Russian Academy of Sciences (Programs of the Presidium of the Russian Academy of Sciences, the Division of Chemistry and Materials Science of the Russian Academy of Sciences, and the Siberian and Ural Branches of the Russian Academy of Sciences, integration grants).

References

1. V. I. Ovcharenko, S. V. Fokin, G. V. Romanenko, Yu. G. Shvedenkov, V. N. Ikorskii, E. V. Tretyakov, and S. F. Vasilevskii, *Zh. Strukt. Khim.,* 2002, **43**, 163 [*Russ. J. Struct. Chem.*, 2002, **43**, 153 (Engl. Transl.)].
2. V. I. Ovcharenko, S. V. Fokin, G. V. Romanenko, V. N. Ikorskii, E. V. Tretyakov, S. F. Vasilevsky, and R. Z. Sagdeev, *Mol. Phys.*, 2002, **100**, 1107.
3. S. Fokin, V. Ovcharenko, G. Romanenko, and V. Ikorskii, *Inorg. Chem.*, 2004, **43**, 969.
4. V. I. Ovcharenko, K. Yu. Maryunina, S. V. Fokin, G. V. Romanenko, and V. N. Ikorskii, *Izv. Akad. Nauk, Ser. Khim.*, 2004, 2304 [*Russ. Chem. Bull., Int. Ed.*, 2004, **53**, 2406].
5. P. Rey and V. I. Ovcharenko, *Spin Transition Phenomena*, in *Magnetism: Molecules to Materials IV*, Eds J. S. Miller and M. Drillon, Wiley-VCH, Weinheim, 2003.
6. E. Tretyakov, S. Fokin, G. Romanenko, V. Ikorskii, S. Vasilevsky, and V. Ovcharenko, *Inorg. Chem.*, 2006, **45**, 3671.
7. *Cambridge Structural Database, Version 5.27*, November 2005 (Updates August 2006).
8. A. Caneschi, P. Chiesi, L. David, F. Ferraro, D. Gatteschi, and R. Sessoli, *Inorg. Chem.*, 1993, **32**, 1445.
9. C. Sporer, K. Wurst, D. B. Amabilino, D. Ruiz-Molina, H. Kopacka, P. Jaitner, and J. Veciana, *Chem. Commun.*, 2002, 2342.
10. D. Philp and J. F. Stoddart, *Angew. Chem., Int. Ed.*, 1996, **35**, 1154.
11. B. Moulton, J. Lu, and M. J. Zaworotko, *J. Am. Chem. Soc.*, 2001, **123**, 9224.
12. E. V. Tretyakov, S. E. Tolstikov, G. V. Romanenko, Yu. G. Shvedenkov, R. Z. Sagdeev, and V. I. Ovcharenko, *Izv. Akad. Nauk, Ser. Khim.*, 2005, 2105 [*Russ. Chem. Bull., Int. Ed.*, 2005, **54**, 2169].
13. I. V. Ovcharenko, Yu. G. Shvedenkov, R. N. Musin, and V. N. Ikorskii, *Zh. Strukt. Khim.,* 1999, **40**, 36 [*Russ. J. Struct. Chem.*, 1999, **40** (Engl. Transl.)].

Received December 18, 2006